

TURBULENCE INTENSITY AND TIME-MEAN VELOCITY DISTRIBUTIONS IN LOW REYNOLDS NUMBER TURBULENT PIPE FLOWS

W. T. PENNELL, E. M. SPARROW and E. R. G. ECKERT

Heat Transfer Laboratory, Department of Mechanical Engineering, University of Minnesota, Minneapolis, Minnesota, U.S.A.

(Received 14 June 1971 and in revised form 4 October 1971)

Abstract—Measurements of the cross-sectional distributions of axial turbulence intensity and time-mean velocity in hydrodynamically developed pipe flows were made by means of a hot-film anemometer. The investigation was concerned with the low Reynolds number turbulent regime, and experiments were performed for five Reynolds numbers between 3200 and 24000. Air was the working fluid. The present measurements, taken together with those of Laufer for high Reynolds number pipe flows (up to 500000), establish that in the near-wall region characterized by y^+ up to 25, the ratio of turbulence intensity to friction velocity is independent of Reynolds number. This same relative turbulence intensity is also independent of the Reynolds number in the neighborhood of the pipe centerline. The measured time-mean velocity distributions deviate more and more from the universal u^+, y^+ profile with decreasing Reynolds number below 10000, which corroborates the findings of previous investigations.

NOMENCLATURE

- Re , Reynolds number, $\bar{u}(2r_0)/\nu$;
- Re_c , Reynolds number based on centerline velocity, $u_c(2r_0)/\nu$;
- r , radial coordinate, measured from centerline;
- r_0 , tube radius;
- u , time-mean axial velocity;
- u_c , centerline velocity;
- \bar{u} , cross-sectionally averaged, time-mean velocity;
- u^+ , dimensionless velocity, u/v^* ;
- u' , axial fluctuation velocity;
- v^* , friction velocity;
- y , radial coordinate, measured from wall;
- y^+ , dimensionless coordinate, yv^*/ν ;
- ν , kinematic viscosity;
- ρ , density;
- τ_w , wall shear.

INTRODUCTION

RECENT studies of low Reynolds number, turbulent pipe flows have been stimulated both

by interest in the basic fluid mechanics and by applications to heat exchange devices. For example, many present-day heat exchangers operate in the low Reynolds number turbulent regime. References [1-5] are representative of the current literature, and additional publications are cited in the bibliographies contained therein. Most of the reported measurements are of the time-mean velocity field. These measurements reveal deviations from the condition of developed turbulence which prevails at moderate and high Reynolds numbers. Specifically, when measured time-mean velocity profiles are plotted on the familiar u^+, y^+ dimensionless coordinates, the data fall above the universal profile over a large portion of the tube cross section. The extent of the deviations increases with decreasing Reynolds number, that is, the u^+, y^+ profiles are Reynolds number dependent.

Although the behavior of the time-mean velocity field is well documented, there appears to be little information on the structure of the turbulence field in the low Reynolds number

turbulent regime. This paper reports the results of measurements of axial turbulence intensity for hydrodynamically developed airflow in a smooth, circular tube. Cross-sectional distributions of turbulence intensity were determined by means of a hot-film anemometer for Reynolds numbers of 3200, 4340, 5850, 11 400 and 24 000. The results were compared with those of Laufer [6] (which correspond to Reynolds numbers of 50 000 and 500 000) with a view toward establishing the dependence of the turbulence intensity on the Reynolds number of the flow. Time-mean velocity profiles were also measured and were compared with the universal profile and with an analytical prediction.

EXPERIMENTAL APPARATUS

The measurements were performed in a smooth, seamless brass tube, 35.5 mm dia., which was carefully aligned and supported to avoid possible secondary flows due to curvature of the tube axis. Clean compressed air, free of oil and water, was provided by a building air supply and delivered to a plenum chamber situated at the upstream end of the test section tube. The air passed from the plenum into the tube via a sharp-edged entrance. All data were collected in a cross section situated 88 diameters from the inlet and two diameters from the downstream end of the test section tube.

A hot-film anemometer was employed to carry out the turbulence and velocity field measurements.* The probe was introduced into the flow through the downstream end of the test section tube. To support and guide the probe traversing mechanism, an extension tube, 35.5 mm dia. and approximately 22 diameters in length, was affixed to the downstream end of the test section tube.

A hot-film sensor was chosen in preference to

a hot-wire sensor because of its greater strength and lesser susceptibility to breakage and because of its shorter sensing length, which affords better spatial resolution. The sensor used in these experiments had a diameter of 0.025 mm, an effective sensing length of 0.25 mm, and an overall length of 0.75 mm. It was installed in the probe holder so that its axis was perpendicular both to the direction of radial traverse and to the streamwise direction. This orientation was chosen both to allow measurements to be made closer to the wall and to minimize variations of velocity along the sensing surface. At the measuring station nearest the tube wall, the wall-to-sensor distance was about 1.25 mm. In view of the fact that the sensor diameter was 0.025 mm, spatial resolution along the direction of radial traverse was quite satisfactory.

The prongs to which the sensor was attached were oriented in the streamwise direction. The calibration of the sensor is described elsewhere [7].

The traversing of the probe across the cross section was accomplished by means of a mechanism situated in the aforementioned downstream extension tube. Figure 1 is a schematic diagram of the traversing apparatus, which is seen to be, in essence, a symmetrical four-bar mechanism wherein the probe arm AE and the driving arm DF are connected through a driving linkage CD. The probe arm pivots about Point A and moves in response to movements of the driving micrometer. It was verified by direct observations with a travelling microscope that the movement of the sensor was within 0.02 mm of that indicated by the driving micrometer. The radial position of the sensor was based on the distance from the tube wall, which was established with the aid of an electrical contact mechanism [7].

The support tube AB of the traversing mechanism was positioned to coincide with the centerline of the downstream extension tube by means of rigid and spring struts. The traversing mechanism could be rotated about AB, thereby permitting radial traverses to be made at any circumferential location. In the present experi-

* The data acquisition system consisted of a Thermo Systems Model 1275 miniature probe equipped with a model 10A cylindrical hot-film sensor and used in conjunction with a Thermo Systems 1050 series constant temperature anemometer.

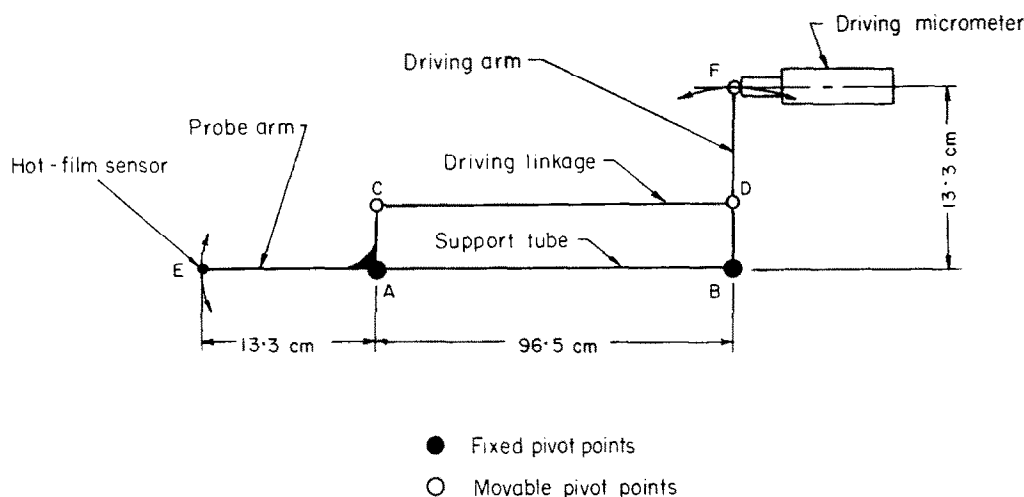


FIG. 1. Schematic diagram of the apparatus for traversing

ments, traverses were made along four radial lines spaced at 90 degree intervals around the circumference. Each of the data points appearing in the subsequent presentation of results represents an average over the four circumferential locations. In general, circumferential asymmetries were small.

The experimental data were reduced by means of a hybrid computer in on-line operation. The hybrid system consisted of an EAI 680 analog computer coupled through an analog-digital interface to a CDC 1700 digital computer. The analog computer was used primarily as a variable time constant RMS voltmeter. The digital computer was programmed to operate the analog computer; to collect, store, and print out the raw data; to perform the necessary calculations required to convert the raw data into the desired physical quantities; and to print out these results.

Upon arriving at the analog computer, the voltage signal from the anemometer was subdivided into two parts. One part was fed to an integrator, where it was averaged over a ten-second interval and then sent to the analog-to-

digital conversion line to be read by the digital computer. The other part went to a filter to eliminate the d-c component. The output signal of the filter was squared, integrated for ten seconds, and the square root taken of the result, which was sent to the digital computer. The levels of the voltage signals processed by the various elements of the analog computer were controlled through the use of amplifiers and scale factors which were set on voltage dividers.

At each measurement station in the flow, four successive determinations of the mean velocity and turbulence intensity were made and averaged. These local averages were subsequently circumferentially averaged as explained previously.

The determination of turbulence intensities from the measured root-mean-square fluctuating voltage signals was performed by a linearized analysis, standard in hot wire and hot film anemometry. This type of analysis is known to overestimate the turbulence intensity at measurement stations where the root-mean-square fluctuation velocity is not small compared with the time-mean velocity. In the case of pipe flows, such stations are situated adjacent to the wall.

RESULTS AND DISCUSSION

Time-mean velocity distributions

To begin the presentation of results, the time-mean velocity distributions will be treated first in order to provide continuity with available information. In this connection, the familiar u^+, y^+ variables are used, where

$$u^+ = u/v^*, \quad y^+ = yv^*/\nu, \quad v^* = \sqrt{(\tau_w/\rho)} \quad (1)$$

in which u is the local time-mean axial velocity, y is the radial distance from the tube wall, and v^* is the friction velocity. The wall shear τ_w appearing in the latter was evaluated from the Blasius relation ($c_f = 0.3164/Re^{1/2}$), which was confirmed to within 7 per cent by means of pressure drop measurements at all of the Reynolds numbers investigated. The cross-sectionally averaged, time-mean velocity needed in the evaluation of the Reynolds number was determined by integration of the measured profiles.

The experimental results are presented on semi-logarithmic coordinates in Fig. 2. The solid

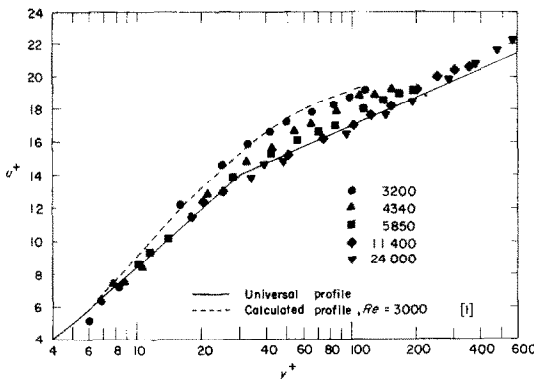


FIG. 2. Time-mean velocity distributions.

line appearing in the figure is the universal velocity profile according to von Kármán [8], the equations for which are

$$u^+ = y^+, \quad y^+ \leq 5 \quad (2a)$$

$$u^+ = 5.0 \ln y^+ - 3.05, \quad 5 \leq y^+ \leq 30 \quad (2b)$$

$$u^+ = 2.5 \ln y^+ + 5.5, \quad y^+ \geq 30. \quad (2c)$$

The significance of the dashed line will be discussed shortly.

Inspection of the figure reveals that at the Reynolds numbers of 11400 and 24000, there is very good agreement between the experimental points and the universal profile. However, at the lower Reynolds numbers, agreement between the data and the universal profile is more and more restricted to the near-wall region of the flow. At locations farther from the wall, the upward deviations of the data from the universal profile become more marked as the Reynolds number decreases.

The just-discussed behavior of the time-mean velocity field is in accord with the findings of prior investigators. The deviations which occur in the low Reynolds number range may be made plausible by examining the basis of the universal velocity profile. In the so-called fully turbulent regime, usually taken as $y^+ > 30$, it is generally assumed that the viscous contribution to the shear stress is negligible. However, with decreasing values of Reynolds number below 10000, the relative importance of the viscous contribution increases and the region of its influence extends farther and farther from the wall. Correspondingly, greater deviations from the universal profile are to be expected as the Reynolds number decreases.

The dashed line in Fig. 2 represents a velocity profile for $Re = 3000$ computed by H. C. Reynolds and co-workers [1] using an eddy viscosity model deduced from their time-mean velocity measurements. The agreement between the present data and the calculated profile is seen to be very good, thereby lending support to the eddy viscosity model of the computations.

For all of the data shown in Fig. 2, the output of the hot-film anemometer was monitored continuously on an oscilloscope, and no intermittency in the turbulence was observed at any Reynolds number.

Turbulence intensity

The only published information known to the authors on turbulence intensity in low Reynolds

number pipe flow is restricted to the pipe centerline. Measurements performed with a hot-wire anemometer [9] and with laser-Doppler systems [10, 11] have been reported. The prior results were brought together by Goldstein and Kreid [10] and are shown in Fig. 3 along with the data

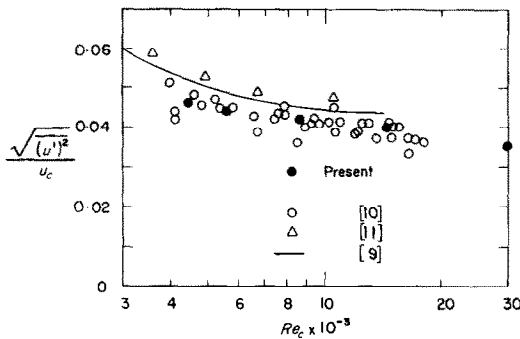


FIG. 3. Turbulence intensity at the pipe centerline.

of the present investigation. The ordinate is the relative axial turbulence intensity at the tube centerline, with the root-mean-square of the fluctuation velocity u' being made dimensionless by the time-mean centerline velocity u_c . The abscissa is the Reynolds number Re_c based on the centerline velocity u_c .

The data shown in Fig. 3 appear to concur in indicating an increase in the relative turbulence intensity at the centerline as the Reynolds number decreases, an outcome which might not have been expected in advance. There is a moderate spread among the results from the different investigators. The generally satisfactory agreement of the present data with the prior results shown in Fig. 3 lends confidence to the measurement technique and instrumentation used herein.

Profiles of axial turbulence intensity are presented in Fig. 4. The distribution of the root-mean-square fluctuating velocity for each Reynolds number is normalized by the corresponding friction velocity v^* . The abscissa variable is the dimensionless radial coordinate r/r_0 (r = radial coordinate, r_0 = tube radius).

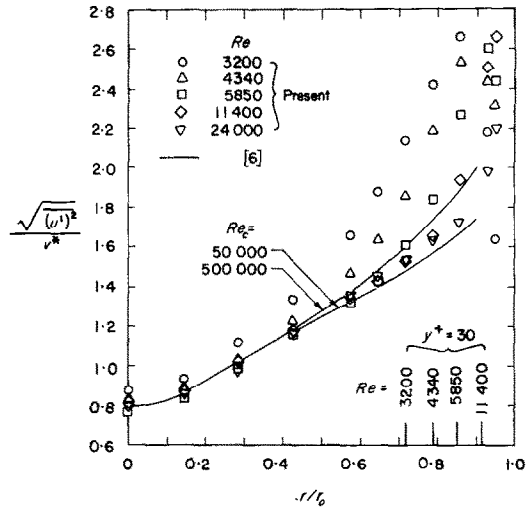


FIG. 4. Turbulence intensity distributions plotted as a function of the radial coordinate.

Also included in the figure are lines representing the data of Laufer [6] for centerline Reynolds numbers Re_c of 50 000 and 500 000. In view of the fact that the data in Fig. 4 cover a Reynolds number range from 3200 to 500 000, the excellent correlation of the turbulence characteristics in the central portion of the tube may be regarded as remarkable. The spread among the data becomes greater in the outer half of the tube cross section. This spread can be traced to the influence of the near-wall regions of the flow.

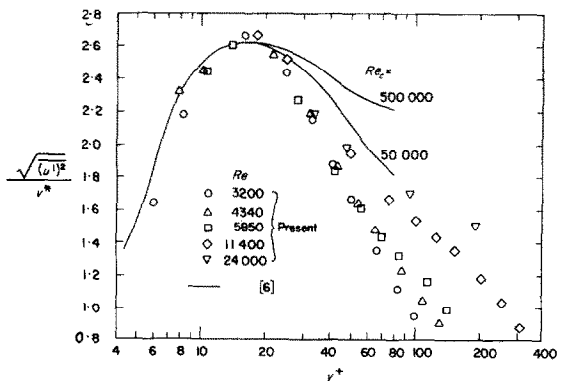


FIG. 5. Turbulence intensity distributions plotted as a function of y^+ .

To give an indication of the extent of the near-wall region, the location of the edge of the von Kármán buffer layer ($y^+ = 30$) is indicated along the abscissa of Fig. 4 for several Reynolds numbers. Clearly, the near-wall region cannot be regarded as a thin layer in a low Reynolds number flow.

To seek a correlation of the turbulence characteristics in the immediate neighborhood of the wall, $\sqrt{[(u')^2]}/v^*$ is plotted as a function of y^+ . Figure 5 contains the data of the present investigation as well as those of Laufer. There is excellent correlation of the results for y^+ values up to 25 for all Reynolds numbers, with the maximum value of the intensity being attained at $y^+ = 17$ or 18. Thus, there appears to be a law of the wall for the turbulence intensity. Beyond $y^+ = 25$, the distributions for the various Reynolds numbers begin to fan out. This fanning out is seen also to occur in the high Reynolds number regime investigated by Laufer. That is, even for high Reynolds numbers, the law of the wall for the turbulence intensity is restricted to y^+ values up to 25. This is to be contrasted with the universal u^+, y^+ distribution for the time-mean velocity (Fig. 2), which, for high Reynolds numbers, is valid over a much larger range of y^+ .

The just-encountered law of the wall for the turbulence intensity can be shown to be plausible on theoretical grounds. There is a layer near the wall where the rates of turbulence production and dissipation are nearly in balance [12]. According to Prandtl [13], the production and dissipation terms can be respectively represented as

$$C_1(u')^2 \frac{du}{dy} \quad \text{and} \quad C_2(u')^2 \frac{1}{l} \quad (3)$$

in which l is a mixing length and C_1 and C_2 are presumed to be constants. Upon equating production and dissipation and introducing the u^+, y^+ variables from equation (1), there follows

$$\frac{\sqrt{[(u')^2]}}{v^*} = \frac{C_1}{C_2} l^+ \frac{du^+}{dy^+} \quad (4)$$

In those regions of the flow where l^+ and u^+ depend primarily on y^+ and are relatively insensitive to the Reynolds number, equation (4) indicates that $\sqrt{[(u')^2]}/v^*$ should very nearly be a universal function of y^+ . Very near the wall, du^+/dy^+ is nearly a constant whereas l^+ increases with y^+ ; correspondingly, $\sqrt{[(u')^2]}/v^*$ increases. In the von Kármán buffer layer, the decrease of du^+/dy^+ with y^+ tends to counteract the increase in l^+ , giving rise to the possibility of a maximum in $\sqrt{[(u')^2]}/v^*$. The experimental results of Fig. 5 exhibit the just-mentioned trends in the near-wall region.

CONCLUDING REMARKS

The present low Reynolds number measurements and those of Laufer for high Reynolds numbers indicate certain regions where the relative axial turbulence intensity $\sqrt{[(u')^2]}/v^*$ is universal (i.e. independent of Reynolds number). Near the tube wall, a law of the wall for the relative turbulence intensity holds, provided that y^+ is used as the correlating coordinate. The correlation applies for y^+ values up to about 25, whereafter the relative turbulence intensity becomes Reynolds number dependent. Even for high Reynolds numbers, the correlation is restricted to $y^+ \sim 25$. The relative turbulence intensity is also independent of Reynolds number in the neighborhood of the tube centerline.

For the time-mean velocity distribution, the validity of the universal u^+, y^+ correlation is eroded away as the Reynolds number decreases below 10 000. In the low Reynolds number range, the upward deviations of the data from the universal profile become more marked with decreasing Reynolds number.

ACKNOWLEDGEMENT

This research was sponsored by Project N00014-68-A-0141-0001, administered by the Office of Naval Research.

REFERENCES

1. H. C. REYNOLDS, M. E. DAVENPORT and D. M. McELIGOT, Velocity profiles and eddy diffusivities for fully developed, turbulent, low Reynolds number flow, Amer. Soc. Mech. Engrs paper no. 68-WA/FE-34 (1968).
2. D. M. McELIGOT, L. W. ORMAND and H. C. PERKINS, Internal low Reynolds number turbulent and transitional gas flow with heat transfer, *J. Heat Transfer* **88**, 239 (1966).
3. H. C. REYNOLDS, T. B. SWEARINGEN and D. M. McELIGOT, Thermal entry for low Reynolds number turbulent flow, *J. Basic Engng* **91**, 67 (1969).
4. C. J. LAWN, Turbulent heat transfer at low Reynolds numbers, *J. Heat Transfer* **91**, 532 (1969).
5. V. C. PATEL and M. R. HEAD, Some observations on skin friction and velocity profiles in fully developed pipe and channel flows, *J. Fluid Mech.* **38**, 181 (1969).
6. J. LAUFER, The structure of turbulence in fully developed pipe flow, NACA report 1174 (1954).
7. W. T. PENNELL, The effect of uniform mass injection on the structure of turbulent flow through a porous pipe, Ph.D. Thesis, University of Minnesota, Minneapolis, Minnesota (1970).
8. T. VON KÁRMÁN, The analogy between fluid friction and heat transfer, *Trans. Am. Soc. Mech. Engrs* **61**, 705 (1939).
9. P. J. BOURKE, D. T. PULLING, L. E. GILL and W. H. DENTON, The measurement of turbulent velocity fluctuations and turbulent temperature fluctuations in the supercritical region by a hot-wire anemometer and a cold wire resistance thermometer, Symposium on Heat Transfer and Fluid Dynamics of Near Critical Fluids, Inst. Mech. Engrs London, paper no. 9 (1968).
10. R. J. GOLDSTEIN and D. K. KREID, Fluid velocity measurement from the Doppler shift of scattered laser radiation, Heat Transfer Laboratory, Department of Mechanical Engineering, University of Minnesota, Minneapolis, Minnesota, report no. 85 (1968).
11. E. B. PIKE, D. A. JACKSON, P. J. BOURKE and D. I. PAGE, Measurement of turbulent velocities from the Doppler shift in scattered laser radiation, *J. Scient. Instrum.* **1**, 727 (1968).
12. A. A. TOWNSEND, Equilibrium layers and wall turbulence, *J. Fluid Mech* **11**, 97 (1961).
13. L. PRANDTL, Über ein neues Formelsystem für die ausgebildete Turbulenz, *Nachrichten von der Akademie der Wissenschaften in Göttingen*, p. 6 (1945).

DISTRIBUTIONS D'INTENSITÉ DE TURBULENCE ET DE VITESSE MOYENNE DANS DES ÉCOULEMENTS TURBULENTS À L'INTÉRIEUR DE TUBES POUR DES NOMBRES DE REYNOLDS FAIBLES

Résumé—On a fait, à l'aide d'un anémomètre à film chaud, des mesures de distribution dans une section droite d'intensité de turbulence axiale et de vitesse moyenne temporelles pour des écoulements hydrodynamiquement développés dans un tube. L'étude concerne le régime turbulent à bas nombre de Reynolds et des expériences ont été menées pour cinq nombres de Reynolds compris en 3200 et 24000. Le fluide considéré est l'air. Les mesures décrites rassemblées avec celles de Laufer pour des écoulements dans des tubes à grand nombre de Reynolds (jusqu'à 500 000) établissent que dans la région proche de la paroi caractérisée par y^+ atteignant 25, le rapport de l'intensité de turbulence à la vitesse de frottement est indépendant du nombre de Reynolds. Cette intensité relative de turbulence est aussi indépendante du nombre de Reynolds dans le voisinage de l'axe central du tuyau. Les distributions de vitesses moyennes temporelles mesurées s'écartent de plus en plus du profil universel u^+ , y^+ quand le nombre de Reynolds décroît au-dessous de 10 000, ce qui confirme les résultats d'études antérieures.

TURBULENZINTENSITÄT UND MITTLERE GESCHWINDIGKEITSVERTEILUNG DER TURBULENTEN ROHRSTRÖMUNG BEI NIEDRIGEN REYNOLDS-ZAHLEN.

Zusammenfassung—Mit Hilfe eines Heissfilmanemometers wurde die radiale Verteilung der axialen Turbulenzintensität und die mittlere Geschwindigkeit in einer hydrodynamisch eingelaufenen Rohrströmung bestimmt. Die Untersuchungen wurden im turbulenten Gebiet durchgeführt, bei 5 Reynolds-Zahlen zwischen 3200 und 24000. Als Fluid wurde Luft verwendet. Die vorliegenden Messungen zusammen mit denen von Laufer für die Rohrströmung bei grossen Reynolds-Zahlen (bis zu 500 000) zeigen, dass in der wandnahen Zone bis zu $y^+ = 25$ das Verhältnis der Turbulenzintensität zur Reibungsgeschwindigkeit unabhängig von der Reynolds-Zahl ist. Diese relative Turbulenzintensität ist auch in der Nähe der Rohrachse unabhängig von der Reynolds-Zahl. Die gemessenen, über die Zeit gemittelten Geschwindigkeitsverteilungen weichen mit abnehmender Reynolds-Zahl, unter 10 000, mehr und mehr von dem universellen Profil u^+ , y^+ ab. Diese Tatsache bestätigt die Aussagen früherer Untersuchungen.

РАСПРЕДЕЛЕНИЯ ИНТЕНСИВНОСТИ ТУРБУЛЕНТНОСТИ И ОСРЕДНЕННОЙ
СКОРОСТИ ТУРБУЛЕНТНОГО ТЕЧЕНИЯ В ТРУБЕ ПРИ МАЛЫХ
ЗНАЧЕНИЯХ ЧИСЛА РЕЙНОЛЬДСА

Аннотация—С помощью пленочного термоанемометра проводились измерения профилей продольной интенсивности турбулентности и осредненной по времени скорости гидродинамически развитого течения в трубе.

Исследовался турбулентный режим при низких значениях числа Рейнольдса от 3200 до 24 000. В качестве рабочей среды использовался воздух. Измерениями, проведенными в настоящей работе, вместе с измерениями Лауфера течений в трубе при больших значениях числа Рейнольдса (до 500 000) было установлено, что в пристеночной области, характеризуемой значениями y^+ до 25, отношение интенсивности турбулентности к скорости трения не зависит от числа Рейнольдса. Относительная интенсивность турбулентности по оси трубы также не зависит от числа Рейнольдса. При уменьшении числа Рейнольдса ниже 10 000 измеренное распределение средней по времени скорости всё больше отклоняется от универсального профиля u^+ , y^+ , что соответствует данным предыдущих исследований.